Fish and Shellfish Immunology 86 (2019) 301–310

Contents lists available at ScienceDirect

Fish and Shellfish Immunology

journal homepage: www.elsevier.com/locate/fsi

Full length article

Identification of thioredoxin domain-containing protein 17 from big-belly seahorse *Hippocampus abdominalis*: Molecular insights, immune responses, and functional characterization

D.S. Liyanage[a], W.K.M. Omeka[a], Hyerim Yang[a], G.I. Godahewa[a], Hyukjae Kwon[a], Bo-Hye Nam[b], Jehee Lee[a,*]

[a] Department of Marine Life Sciences & Fish Vaccine Research Center, Jeju National University, Jeju Self-Governing Province, 63243, Republic of Korea
[b] Biotechnology Research Division, National Institute of Fisheries Science, 408-1 Sirang-ri, Gijang-up, Gijang-gun, Busan, 46083, Republic of Korea

ARTICLE INFO

Keywords:
Antioxidant protein
Hippocampus abdominalis
Redox balance
Temporal expression analysis
Thioredoxin domain-containing protein 17

ABSTRACT

Thioredoxin domain-containing protein 17 (TXNDC17) is a small protein (~14 kDa) involved in maintaining cellular redox homeostasis via a thiol-disulfide reductase activity. In this study, TXNDC17 was identified and characterized from *Hippocampus abdominalis*. The open reading frame (ORF) consisted of 369 bp and 123 amino acids. Similar to the other thioredoxins, TXNDC17 contained a conserved WCXXC functional motif. The highest spatial mRNA expressions of *HaTXNDC17* were observed in the muscle, brain, and intestine. Interestingly, the mRNA expression of *HaTXNDC17* in blood showed significant upregulation at 48 h against all the pathogen associated molecular patterns (PAMPs) and bacteria. Further, *HaTXNDC17* transcripts in the trunk kidney were significantly upregulated at 24–48 h by bacterial endotoxin lipopolysaccharides (LPS), viral mimic polyinosinic: polycytidylic acid (poly I:C), and gram-negative bacteria (*Edwardsiella tarda*). The DPPH assay showed that the radical scavenging activity varies in a concentration-dependent manner. The insulin reduction assay demonstrated a significant logarithmic relationship with the concentration of rHaTXNDC17. Moreover, FHM cells treated with recombinant HaTXNDC17 significantly enhanced cellular viability under oxidative stress. Together, these results show that HaTXNDC17 function is important for maintaining cellular redox homeostasis and that it is also involved in the immune mechanism in seahorses.

1. Introduction

Thioredoxins are intracellular proteins ubiquitously found in all the kingdoms of living organisms. The thioredoxin family comprises thiol-transferases, including thioredoxins (Txn) and glutaredoxins (Grx) [1,2]. The thioredoxin domain possesses a universally conserved redox-active thiol disulfide CXXC motif with two cysteines called the thioredoxin motif. The thiol active CXXC motif of the thioredoxin domain is also found in the protein disulfide isomerase (PDI) and PDI-D subfamily [3]. Further, the thioredoxin domain can be found in *Escherichia coli* disulfide-bond oxidoreductases (DsbA, DsbC, DsbD, DsbE, and DsbG), which promote the disulfide bond formation in periplasmic proteins [4].

Thioredoxin domain-containing proteins and thioredoxin-related proteins are ubiquitously expressed in all cellular organelles. For example, thioredoxin reductase 2 (Txnrd2), Txn, glutaredoxin 2 (Grx2), and peroxiredoxin 3 (Prx3) can be found in the mitochondria, while PDI proteins, calcium binding protein 1 (CaBP1), ERp72, thioredoxin-related transmembrane protein (Tmx), and ER-resident protein disulfide reductase/J-domain-containing PDI-like protein (ERdj5/JPDI) are present in the endoplasmic reticulum [5]. Further, nucleoredoxin and Grx2 are expressed in the nucleus. The cytosol contains a large number of thioredoxin-related proteins including Txnrd1, thioredoxin-related protein 32 (Trp32), thioredoxin-like protein 2 (Txnl2), Grx1, Prx1, Prx2, Prx4, Prx5, and Prx6. Apart from that, plasma cell thioredoxin-related protein (PC-Trp), Txnrd3, Txn1, Txn2, and Txn3 show tissue-specific expression [5].

Thioredoxins play multiple functions at the cellular level. They act as reductases and regulate the redox homeostasis, thereby protecting proteins and cellular organelles from oxidative aggregation and inactivation [6–9]. Further, thioredoxins protect the cells from various environmental stresses such as reactive oxygen species (ROS), arsenate,

* Corresponding author. Marine Molecular Genetics Lab, Department of Marine Life Sciences, Jeju National University, Jeju Self-Governing Province, 63243, Republic of Korea.
E-mail address: jehee@jejunu.ac.kr (J. Lee).

https://doi.org/10.1016/j.fsi.2018.11.040
Received 16 June 2018; Received in revised form 12 November 2018; Accepted 15 November 2018
Available online 16 November 2018
1050-4648/

and peroxynitrite [10,11]. Moreover, some thioredoxins promote protein folding [12], modulate inflammatory response [13], and prevent apoptosis [14].

Big-belly seahorse (*Hippocampus abdominalis*) is one of the important seahorse species used in oriental medicine as a remedy for treating diseases such as erectile dysfunction, as well as for suppressing neuroinflammatory responses and collagen release [15,16]. Moreover, it exhibits antitumor and anti-aging properties [15]. Further, it is used as an ornamental fish species and as food [15]. However, seahorses are highly susceptible to pathogenic attacks leading to fatal diseases [17,18], and hence they have been included in the conservation list [19].

Edwardsiella tarda is considered a serious fish pathogen in aquaculture that causes edwardsiellosis in cultured and wild fishes. It can produce virulence factors leading to greater survival of bacteria in the host [20]. Furthermore, *Streptococcus iniae* is a severe fish pathogen that can cause streptococcal disease which influences the mortality of fish [21]. Therefore, exploring the immune mechanisms prevalent in seahorses against these pathogens provides insight into the host's immune system at the molecular level [22,23]. In this study, thioredoxin domain-containing protein 17 from big-belly seahorse (HaTXNDC17) was characterized to gain a better understanding of thioredoxin mechanisms in teleost fishes. According to our knowledge, this is the first comprehensive study of TXNDC17 in fish. Furthermore, cDNA and the protein sequences of HaTXNDC17 were characterized using various bioinformatics tools, the recombinant protein was produced to evaluate the functional aspects using the 2,2-diphenyl-1-picrylhydrazyl (DPPH) assay, insulin disulfide reduction assay, and cell survival assay. Finally, the spatial distribution of the *HaTXNDC17* and temporal transcriptional modulations were investigated against bacterial endotoxin lipopolysaccharides (LPS), viral mimic polyinosinic-polycytidylic acid (poly I:C), gram-negative bacteria (*E. tarda*) and gram-positive bacteria (*S. iniae*) as stressors.

2. Materials and methods

2.1. Identification of cDNA sequences

The cDNA sequence of *HaTXNDC17* was identified from the seahorse transcriptomic database established at Marine Molecular Genetics Lab, Jeju National University. The database was developed using the 454 GS FLX™ sequencing data. The total RNA was isolated from the liver, kidney, gill, spleen and blood tissues using 18 seahorses. Extracted RNA was purified using RNeasy Mini kit (Qiagen, USA) and sent for sequencing (Insilicogen, Korea). The method was described in our previous study [24]. The collected sequence was cross-checked and confirmed with the NCBI Blast tool with NCBI nucleotide and non-redundant protein databases [25].

2.2. Bioinformatics analysis

The cDNA sequence of *HaTXNDC17* was analyzed by using several *in silico* tools. Initially, the cDNA sequence of *HaTXNDC17* gene was assessed for the open reading frame (ORF) using the Unipro UGENE bioinformatics software v1.26.1 and the corresponding amino acid sequence was derived according to the best ORF matches. Further, NCBI conserved domain database (NCBI CDD) (https://www.ncbi.nlm.nih.gov/Structure/cdd/wrpsb.cgi), ExPASy Prosite (http://prosite.expasy.org/), and EMBL-EBI Pfam domain database (http://pfam.xfam.org/) were used to determine the characteristic domain structure, active site motif, and the signature motifs in the amino acid sequence. Moreover, molecular properties were figured out by using ExPASy Protparam (http://web.expasy.org/protparam/). Signal peptide and its cleavage site were checked by using SignalP 4.1 online tool (http://www.cbs.dtu.dk/services/SignalP/). All known characteristic motifs of the sequence of TXNDC17 were analyzed by using the Motif Scan software (http://myhits.isb-sib.ch/cgi-bin/motif_scan). Potential *N*-linked glycosylation sites were checked by using the NetNGlyc 1.0 server (http://www.cbs.dtu.dk/services/NetNGlyc/). SWISS model ExPASy protein modeling workbench (https://swissmodel.expasy.org/) was used to draw the predicted tertiary structure of thioredoxin domain and other amino acid residues in the HaTXNDC17. The 3D structure of the proteins was created by using PyMOL v1.3 software. Characteristic motifs and domain structure were illustrated by using IBS 1.0.3 software.

The thioredoxin orthologs were determined from the NCBI public database and compared against each individual sequence using EMBOSS needle software (http://www.ebi.ac.uk/Tools/psa/emboss_needle/) to find their sequence identities and similarities. Online Clustal Omega multiple sequence alignment tool (http://www.ebi.ac.uk/Tools/msa/clustalo/) was used to align the species-specific amino acid sequences. Evolutionary relationship and phylogenetic analysis were carried out by using the MEGA7 tool with a neighbor-joining method with 5000 bootstraps [26].

2.3. Rearing of seahorses and tissue collection

Healthy seahorses were obtained from Marine Ornamental Fish Breeding Center (Jeju Island, Republic of Korea). Seahorses were kept in tanks (300 L) with a controlled environment for one week at 18 ± 2 °C and 34 ± 0.6 practical salinity units (psu). Six healthy seahorses (3 males and 3 females) with an average body weight of 8 g were dissected and fourteen different tissues (ovary, spleen, intestine, gill, liver, testis, skin, muscle, heart, stomach, trunk kidney, pouch, brain and blood) were carefully removed for the tissue distribution analysis. Seahorse blood was collected from the tail and immediately centrifuged at 3000 × *g* for 10 min at 4 °C to isolate the peripheral blood cells. All the samples were stored at −80 °C after immediately frozen by using liquid nitrogen.

For the temporal expression analysis experiment, juvenile big belly seahorses with an average body weight of 3 g were divided into five groups including 30 individuals per tank and they were acclimatized as mentioned in previous paragraph. Seahorses were intraperitoneally injected with 100 μL of LPS (1.25 μg/μL), poly I:C (1.5 μg/μL), *E. tarda*: KCTC12267 (5×10^3 CFU/μL), and *S. iniae*: KCTC3657 (10^5 CFU/μL) dissolved in phosphate buffered saline (PBS - pH 7.4). Brain heart infusion (BHI) growth media with 1.5% salt was used to grow the bacteria at 25 °C until it reached 0.5 OD_{600}. Then the bacteria were harvested by centrifugation at 3500 rpm for 20 min and resuspended in PBS buffer. The control group was injected with 100 μL of PBS. Following the immune stimulation, blood and trunk kidney tissues from five seahorses were isolated at 3 h, 6 h, 12 h, 24 h, 48 h, and 72 h post injection (p.i.). Additionally, five seahorses were dissected at 0 h p.i and these tissues were collected as a control. During the experiment period, seahorses were not fed.

2.4. cDNA library construction

Total RNA was extracted from isolated tissues using RNAiso plus reagent (TaKaRa, Japan) and clean-up with RNeasy spin column (Qiagen, USA) according to the protocol supplied by the manufacturer. Purity and the concentration of the extracted RNA were measured by the spectrophotometer and subsequently visualized on a 1.5% agarose gel. The cDNA was synthesized from 2.5 μg of RNA by using PrimeScript™ II 1st Strand cDNA Synthesis Kit (TaKaRa, Japan). Finally, constructed cDNA libraries were diluted to 40-fold and stored at −80 °C for longer use.

2.5. Spatial and temporal transcriptional analysis

The mRNA expression of the *HaTXNDC17* gene was measured with quantitative real-time PCR (qPCR) by using the TaKaRa Thermal Cycler Dice Real Time System III. Seahorse 40S ribosomal protein S7 gene

Table 1
Primers used in the study.

Primer Sequence 5′–3′	Description	Amplicon size	Tm (°C)	Accession No
GAGAGAcatatgATGGCCCAGTACGAACAAGTG	TXNDC17 Cloning F, *Nde*I	372 bp	57.5 °C	MH455283
GAGAGAgatatcTCAATCTTCAGTGAACATCATCCTCAC	TXNDC17 Cloning R, *Eco*RV	372 bp	56.7 °C	MH455283
CCAGGGCTCGGTCTTCATCTACT	TXNDC17 qPCR F	149 bp	60 °C	MH455283
AGCATTCCTCCTCCACCAGTTTCT	TXNDC17 qPCR R	149 bp	60 °C	MH455283
GCGGGAAGCATGTGGTCTTCATT	40S ribosomal protein S7, qPCR F	95 bp	60 °C	KP780177
ACTCCTGGGTCGCTTCTGCTTATT	40S ribosomal protein S7, qPCR R	95 bp	60 °C	KP780177

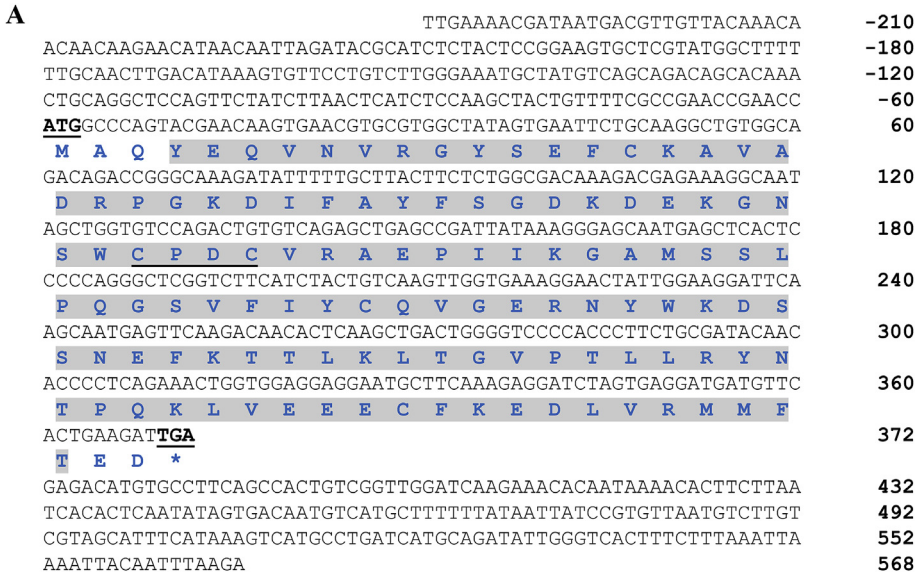

Fig. 1. (A) Nucleotide and deduced amino acid sequence of HaTXNDC17 from big-belly seahorse. Start and stop codons denoted by underlined bold black letters and conserved thioredoxin related protein 14 family domain shaded in ash color. CPDC active site motif represented in blue color underlined letters. Stop signal of the protein denoted by an asterisk mark. (B) Structural representation of the big belly seahorse thioredoxin domain-containing protein 17 (TXNDC17). The CXXC motif is represented by red-colored letters and thioredoxin related protein 14 family domain is shaded in light green. Maps and boundaries are based on the NCBI Conserved Domain Database (CDD). Numbers correspond to the first/last residues in each module. (For interpretation of the references to color in this figure legend, the reader is referred to the Web version of this article.)

Table 2
Pairwise identity and similarity percentages of HaTXNDC17 with its ortholog amino acids.

Accession	Species Name	Identity (%)	Similarity (%)
XP_019748365.1	Tiger tail seahorse (*Hippocampus comes*)	99.2	99.2
XP_004075376.1	Japanese rice fish (*Oryzias latipes*)	78.0	87.0
XP_021443673.1	Rainbow trout (*Oncorhynchus mykiss*)	77.2	87.8
AAI64925.1	Zebrafish (*Danio rerio*)	76.4	88.6
XP_020784309.1	Mudskipper (*Boleophthalmus pectinirostris*)	76.4	87.0
XP_012730006.1	Mummichog (*Fundulus heteroclitus*)	74.8	89.4
XP_020476365.1	Asian swamp eel (*Monopterus albus*)	74.0	90.2
NP_001089800.1	African clawed frog (*Xenopus laevis*)	67.7	81.5
KYO32106.1	American alligator (*Alligator mississippiensis*)	63.4	78.9
OPJ78416.1	Band-tailed pigeon (*Patagioenas fasciata*)	61.8	74.8
XP_003131925.1	Wild boar (*Sus scrofa*)	61.0	77.2
NP_001192750.1	Cattle (*Bos taurus*)	59.3	75.6
NP_116120.1	Human (*Homo sapiens*)	58.5	77.2
NP_001099275.1	Brown rat (*Rattus norvegicus*)	58.5	76.4
NP_001279378.1	Australian ghostshark (*Callorhinchus milii*)	52.8	74.0

(accession no: KP780177) was used as an internal reference gene in the qPCR experiment. The reaction was performed in a 10-μL reaction mixture composed of 50 ng of template cDNA, TaKaRa Ex Taq™ SYBR premix 5 μL with 4 pmol of each primer (Table 1) using a thermal cycler profile of initial denaturation at 95 °C for 10 s and 45 cycles of 95 °C for 5 s, 58 °C for 10 s, and 72 °C for 20 s. The final cycle was set to dissociation analysis using the following cycle: 95 °C for 15 s, 60 °C for 30 s and 95 °C for 15 s.

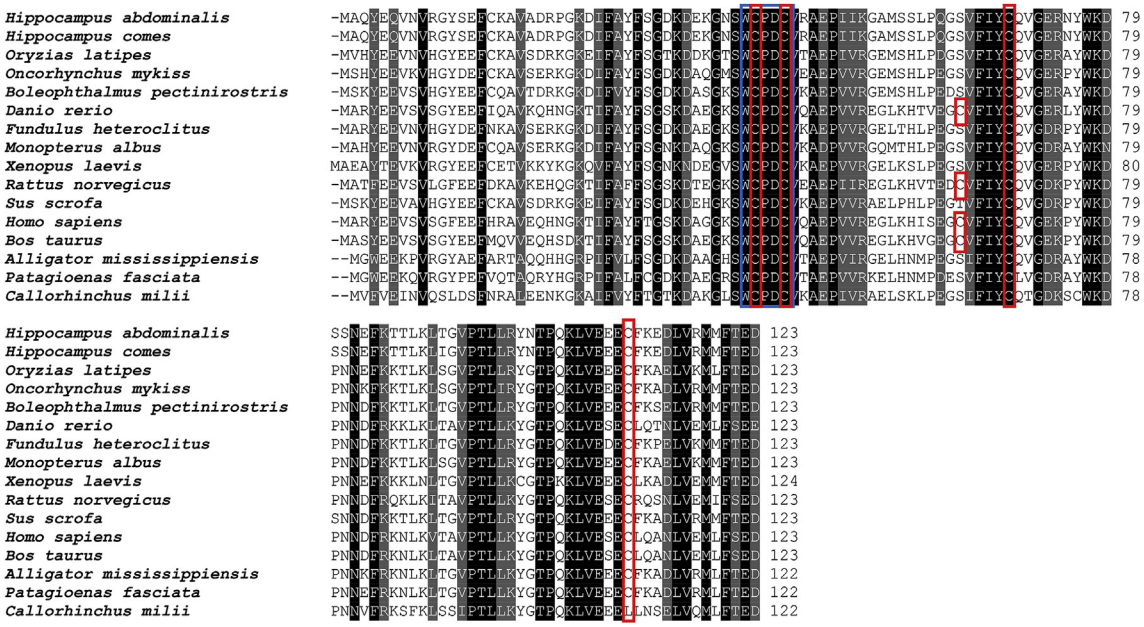

Fig. 2. Comparison of the amino acid sequences of *Hippocampus abdominalis* with their respective counterparts from kingdom Animalia. Conserved cysteine residues are indicated with red-colored boxes and the WCXXC conserved motif is indicated with a blue-colored box. (For interpretation of the references to color in this figure legend, the reader is referred to the Web version of this article.)

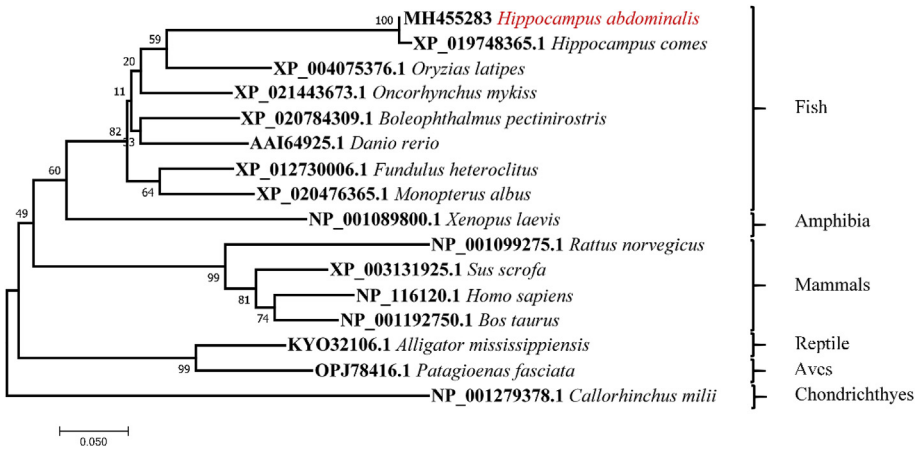

Fig. 3. Phylogenetic tree of big belly seahorse thioredoxin domain-containing protein 17 (TXNDC17) gene. The evolutionary development of each gene was analyzed with its different homologs under different taxonomic groups based on the multiple alignment profile of the protein sequences generated by the neighbor-joining method using MEGA 7.0 software with 5000 bootstraps.

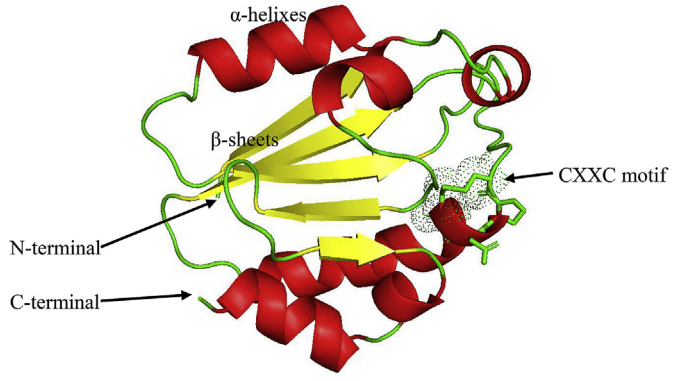

Fig. 4. Predicted tertiary structure of thioredoxin related protein 14 family domain of HaTXNDC17. Catalytic site residues are represented by dotted spheres.

The Livak ($2^{-\Delta\Delta CT}$) method [27] was used to calculate the relative mRNA expression in the qPCR experiment. All the experiments were conducted in triplicate. Spatial expression folds of the *HaTXNDC17* transcripts in different tissues were calculated as fold values relative to mRNA expression levels of the seahorse 40S ribosomal protein S7 gene. Statistical analysis was performed by the analysis of variance (ANOVA) with post-hoc pairwise comparisons. The tissue showing the lowest mRNA expression was used for the basal level. In the temporal expression analysis, the mRNA expression levels of blood and trunk kidney tissues were represented as fold changes relative to the PBS control. Data were calculated in terms of standard deviation (SD); statistical significance was considered at $P < 0.05$.

2.6. Recombinant plasmid construction

cDNA encoding mature information of the HaTXNDC17 was amplified using a 50-μL reaction mixture having 5 units of ExTaq polymerase, 5 μL of 10 × ExTaq buffer, 4 μL of 2.5 mM dNTPs, 0.4 μL of 10 pmol/μL of each primer (Table 1), and 50 ng of template cDNA. The reaction steps consisted of initial denaturation at 94 °C for 3 min, followed by 35 cycles of 94 °C for 30 s, 55 °C for 30 s, 72 °C for 45 s, and a final extension at 72 °C for 10 min. Then PCR product was purified using AccuPrep® PCR purification Kit (Bioneer Co., Korea). PCR amplified HaTXNDC17 gene and the pMAL c5x (BioLabs Inc., USA) cloning

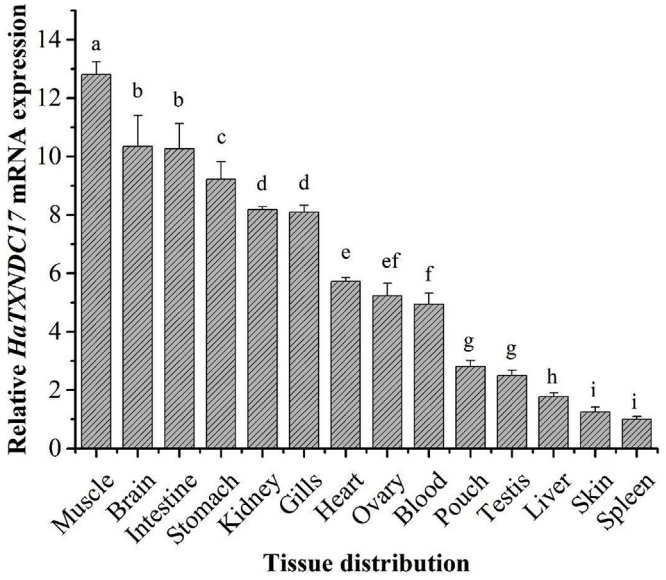

Fig. 5. HaTXNDC17 tissue-specific transcript expression analysis in healthy big belly seahorses under normal physiological conditions. The mRNA expression level of each tissue is indicated relative to the mRNA expression of spleen tissue. Statistical analysis was performed by ANOVA with posthoc pairwise comparisons. The data are represented as mean values (n = 3) ± standard deviation (SD) and $P < 0.05$.

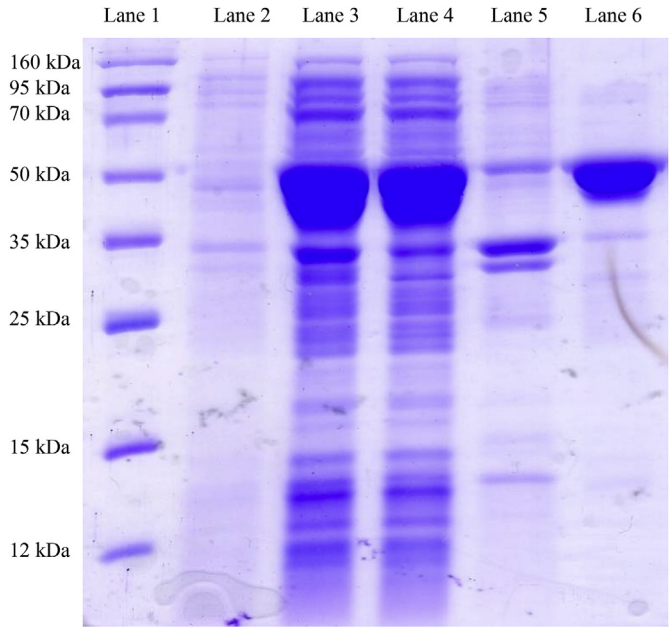

Fig. 7. SDS-PAGE analysis of overexpressed and purified HaTXNDC17 as MBP-fusion protein. Lane 1: protein ladder, Lane 2: crude extract of un-induced *E. coli* ER2523 cells, Lane 3: crude extract of induced *E. coli* ER2523 cells, Lane 4: supernatant after centrifugation, Lane 5: pellet, Lane 6: purified HaTXNDC17 fusion protein.

vector were subjected to double restriction digestion with *Nde*I and *Eco*RV. Then, 200 ng of digested PMAL c5x vector and 50 ng of digested insert fragment were ligated by using 5 μL of Ligation Mighty Mix, (TaKaRa, Japan) followed by a 30-min incubation at 16 °C in a thermal cycler and overnight incubation at 4 °C. The ligated product was transformed into *E. coli* DH5α competent cells by using the heat-shock method. HaTXNDC17 recombinant plasmids were isolated using the AccuPrep Plasmid Mini Extraction Kit (Bioneer Co., Korea) from the grown cell cultures, and the sequence was confirmed by using capillary sequencing (Macrogen, Korea).

2.7. Protein expression and purification

Sequence-confirmed recombinant plasmids were transformed into *E. coli* ER2523 cells (Novagen, Germany). Then, the transformed cells were grown in LB rich media (0.2% glucose + LB) supplemented with 100 μg/mL ampicillin. Cell cultures were incubated at 37 °C and 200 rpm until the OD_{600} value reached 0.5. Protein production was induced by adding 1 mM isopropyl β-D-1-thiogalactopyranoside (IPTG). The cell culture was further incubated at 25 °C and 200 rpm for 8 h. Then, it was centrifuged for 30 min at 3500 rpm, 4 °C, and the cell pellet was resuspended in 25 mL of column buffer containing 20 mM Tris-HCl, 200 mM NaCl and 1 mM EDTA (pH 7.4). Recombinant protein (rHaTXNDC17) was purified as a fusion protein of maltose binding protein (MBP) by PMAL protein fusion and purification system (NEB, USA) according to the manufacturer instructions. Bradford's method [28] was used to measure the concentrations of the purified recombinant proteins, and 12% SDS-PAGE was performed to visualize the protein banding patterns at different stages of purification. Eluted proteins were stored at −80 °C for future use.

2.8. Functional assays

2.8.1. DPPH radical scavenging assay

The 2,2-diphenyl-1-picrylhydrazyl (DPPH) radical scavenging assay [29] was performed in a 96-well plate to determine the radical scavenging ability of rHaTXNDC17. First, 0.4 mM DPPH solution was prepared with dimethylsulfoxide (DMSO). Then, 100 μL of the protein sample at different concentrations (15, 30, 45, 60, and 90 μg/mL) along

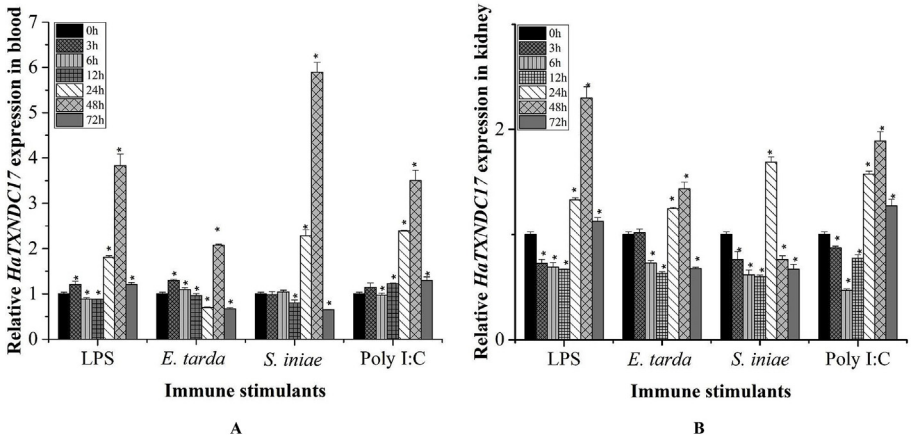

Fig. 6. Temporal expression profiles of *HaTXNDC17* in the blood (A) and kidney (B) tissues after LPS, *E. tarda*, *S. iniae*, and Poly (I:C) challenges. The relative fold changes in expression were compared with those of PBS-injected controls at different time points. The vertical bars represent the mean values (n = 3) ± SD. Significant differences are compared to the blank (0 h) with $P < 0.05$.

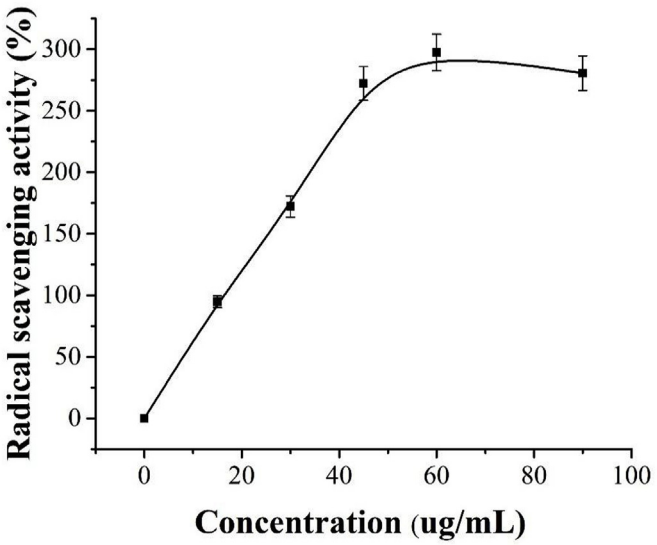

Fig. 8. DPPH radical-scavenging activity of rHaTXNDC17 at different concentrations. Ascorbic acid was used as a standard in the experiment. Data are represented as the mean of triplicates with standard deviation (P < 0.05).

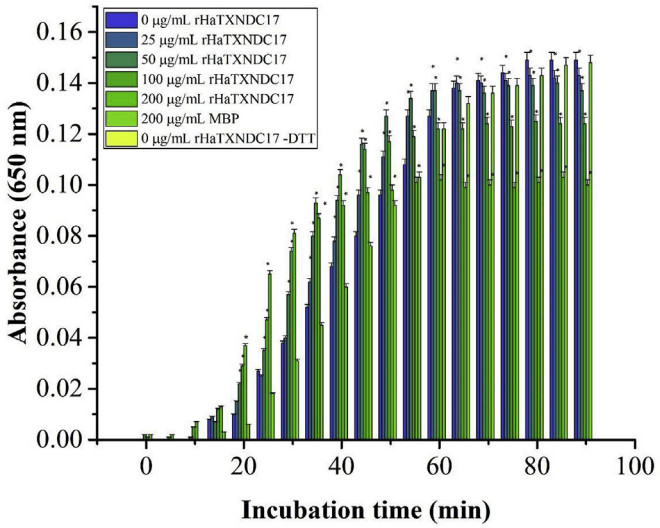

Fig. 9. Insulin disulfide reduction activity assay for rHaTXNDC17. The reaction was performed with 0, 25, 50, 100, and 200 μg/mL rHaTXNDC17 in the presence of DTT. The negative control was prepared in the absence of DTT. The turbidity was monitored at 650 nm and the difference in the absorbance was plotted against the incubation time. Independent student t-test were used to compare the treatments. Standard deviation (SD) was calculated and significant differences were defined at P < 0.05. Data are presented as mean values (n = 3).

with 100 μL of DPPH solution were added into the wells. Ascorbic acid was used as positive control at the above concentrations. Absorbance of the mixture was recorded at 517 nm after 30-min incubation at room temperature. Radical scavenging activity (RSA) percentage was calculated for each treatment according to the following equation: [(Optical density of control - Optical density of sample)/Optical density of control] × 100. The IC_{50} value of HaTXNDC17 for DPPH was measured as described previously [30].

2.8.2. Insulin disulfide reduction assay

Insulin disulfide reduction assay was performed in a 96-well plate to determine the antioxidant activity of rShTXNLDC17 [24]. Total reaction mixture (200 μL) was prepared by adding 10 μL of 2 mM insulin from bovine pancreas, 10 μL of 0.5 M ethylenediaminetetraacetic acid (EDTA) (pH 8.0), and 175 μL of recombinant protein in phosphate buffered saline (PBS) (at 0, 25, 50, 100, and 200 μg/mL), and the reaction was initiated by adding 5 μL of 0.1 M dithiothreitol (DTT). Samples were incubated at 25 °C for 120 min, and absorbance at 650 nm was recorded at 5-min intervals. A negative control was prepared using DTT, without the recombinant protein. In addition, a blank was prepared by adding all the components without DTT. All the samples were prepared in triplicate. The statistical analysis was performed using IBM SPSS statistics 24 software (IBM, USA), and an independent student t-test was used to compare the treatments. Standard deviation (SD) was calculated and significant differences were defined at P < 0.05. The IC_{50} value of HaTXNDC17 in the insulin reduction assay was measured [30]. The specific activity was calculated using the equation (ΔA_{650} nm × min^{-1} × μM^{-1} protein) as described previously [31].

2.8.3. Protective effect on the cultured cells under oxidative stress

Cell viability assay was conducted to investigate the cellular protective ability of rHaTXNDC17 protein. Previous studies had suggested that thioredoxins induce cell survival under oxidative stress [32]. Fathead minnow (FHM) epithelial cells were cultured according to a recommended method using Leibovitz's L-15 medium (ThermoFisher Scientific, USA) with 10% fetal bovine serum (FBS) and 1% penicillin and streptomycin. Initially, FHM cells were seeded at a concentration of 2×10^5/mL in a 96-well plate. Seeded FHM cells were incubated at 25 °C for 24 h. The cells were pre-treated with different concentrations of rHaTXNDC17 (0, 25, 50, 75, and 100 μg/mL) and 1 mM dithiothreitol (DTT) and incubated for 30 min. H_2O_2 (100 μM) was added to the cell culture medium to induce oxidative stress followed by a 24 h incubation. Control samples were prepared without adding 100 μM H_2O_2 to cells. Cellular viability was checked by using the standard 3-(4,5-dimethylthiazol-2-yl)-2, 5-diphenyltetrazolium bromide (MTT) assay. After 24-h incubation, 50 μL of 2 mg/mL MTT solution was added to each well (containing 200-μL reaction mixture) and samples were incubated for 3 h. The supernatants were aspirated and formazan crystals were dissolved by adding 150 μL of DMSO into each well. Finally, absorbance of the reaction mixtures was measured at 540 nm using the SYNERGY/HT™ microplate reader (Biotek, Korea). Microscopic observations of each treatment were recorded using Leica DFC425C digital microscope. Extent of conversion of MTT into insoluble formazan was used to calculate the relative percentage of cell viability. Absorbance of control cells was considered as 100% cell viability. Statistical analysis was performed by an ANOVA with post-hoc pairwise comparisons. All the samples were tested in triplicate (n = 3), and mean percentages ± SD were plotted compared to the control cells.

3. Results

3.1. Bioinformatics analysis of HaTXNDC17 sequence

The cDNA sequence of *HaTXNDC17* was identified from the seahorse transcriptome database and the sequence was deposited in the NCBI GenBank under the accession no: MH455283. The ORF of *HaTXNDC17* was 369-bp long and comprised of 123 amino acids (aa). *In silico* analysis revealed that the estimated molecular mass and predicted isoelectric point (*pI*) was 14.1 kDa and 5.04, respectively. HaTXNDC17 did not possess signal peptide and *N*-linked glycosylation sites. According to the Conserved Domain Database (NCBI) search results, HaTXNDC17 contained thioredoxin domain between 4 and 121 aa residues and conserved redox-active motif (Cys-X-X-Cys) between 43 and 46 aa (Fig. 1).

3.1.1. Homology and phylogenetic analysis

According to pairwise alignment, HaTXNDC17 showed the highest

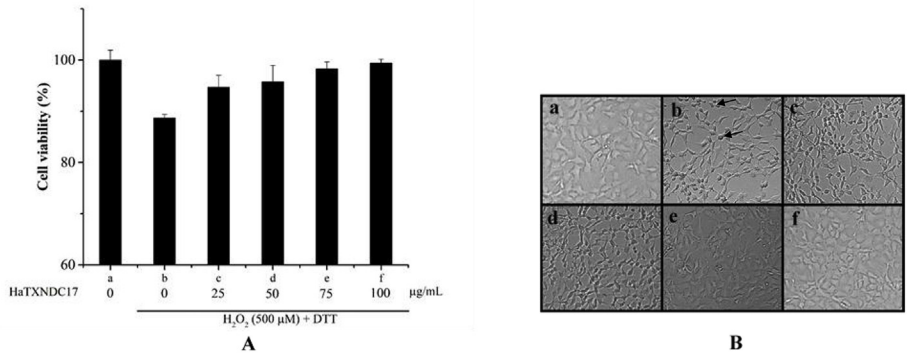

Fig. 10. (A) Effects of rHaTXNDC17 on viability of fathead minnow epithelial cells (FHM) exposed to 100 µM H2O2. (B) Microscopic observations of FHM cells with related to each treatment and black arrows indicate damaged cells. Treatments: (a) control cells; (b) cells treated with H2O2 (100 µM), (c–f) cells pretreated with 25–100 µg/mL of rHaTXNDC17 and 1 mM of DTT followed by 100 µM of H_2O_2. Statistical analysis was performed by ANOVA with posthoc pairwise comparisons. All the samples were treated in triplicate (n = 3) and mean percentages ± SD were plotted.

identity and similarity of 99.2% with *Hippocampus comes* (Table 2). A multiple sequence alignment demonstrated that cysteine residues in the WCXXC motif were conserved among all of the selected species and were represented as WCPDC in fish. Further, folding sites and catalytic sites were highly conserved across all species. There were five conserved cysteines in mammals while teleost had four (Fig. 2). According to the phylogenetic tree, orthologs from different classes of the animal kingdom clustered to their original taxonomic subgroups, and positioned within the teleost group, showing the closest relationship with others (Fig. 3).

3.1.2. Protein structure

The tertiary structure of HaTXNDC17 was modeled by using the structure of closely matched PDB template 1wou.1 (Fig. 4); HaTXNDC17 showed 77% similarity with the template. In terms of domain structure, HaTXNDC17 consisted of thioredoxin domain, whose active site motif was located at the beginning of the second α-helix. Further, the tertiary structure of HaTXNDC17 had a central core consisting of five β-sheets surrounded by five α-helixes. HaTXNDC17 showed very similar three-dimensional structure to human TXNDC17 with slight alterations.

3.1.3. mRNA expression analysis

Spatial expression profile of *HaTXNDC17* under normal physiological conditions was observed in 14 different tissues. The lowest mRNA expression level of *HaTXNDC17* was detected in the spleen (1.00 ± 0.09-fold) and the highest expression level was observed in the muscle (12.80 ± 0.43-fold), followed by the brain (10.33 ± 1.06-fold), the intestine (10.25 ± 0.87-fold), the stomach (9.21 ± 0.60-fold), and the trunk kidney (8.17 ± 0.09-fold) (Fig. 5).

Immune-responsive transcriptional modulation of the *HaTXNDC17* gene was monitored for two different immune-related tissues. The temporal expression profile of *HaTXNDC17* in the blood showed significant up-regulation 24 h p.i. against LPS, *S. iniae,* and poly I:C stressors. Moreover, *HaTXNDC17* expression was significantly upregulated at 48 h p.i. against all of the bacteria and PAMPs (Fig. 6A). In the trunk kidney tissues, *HaTXNDC17* transcripts were significantly upregulated between 24 and 48 h p.i. in response to all of the stressors except in *S. iniae*. The LPS, *E. tarda* and poly I:C injected samples reached a peak at 48 h during the experiential time, whereas *HaTXNDC17* expression in *S. iniae* treated samples showed upregulation at 24 h p.i. and gradually decreased thereafter over time (Fig. 6B).

3.1.4. Protein expression and purification of rHaTXNDC17

The molecular weight of the HaTXNDC17 protein is approximately 14.1 kDa. Together with the MBP fusion protein (~42.5 kDa), rHaTXNDC17 showed protein band at ~ 56.6 kDa in an SDS-PAGE gel, which agreed with the expected molecular weight of rHaTXNDC17 (Fig. 7).

3.2. Functional assays

3.2.1. DPPH assay

Fig. 8 shows the percentage of DPPH radical scavenging activity of rHaTXNDC17 compared to that of ascorbic acid as a reference compound. A concentration-dependent relationship can be observed in the DPPH radical scavenging capacity that is increased with concentrations. The protein showed maximum inhibition of DPPH radicals (14.76%) within the concentration range used. Significant scavenging ($P < 0.05$) of free radicals was evidenced at all the concentrations tested with rHaTXNDC17 and the reference (0–90 µg/mL). Further, rHaTXNDC17 showed IC_{50} value at the concentration of 23.94 µg/mL.

3.2.2. Insulin disulfide reduction assay

The biological activity of rHaTXNDC17 was evaluated using insulin disulfide reduction assay. Presence of rHaTXNDC17 increased the rate of insulin reduction that was detectable after 10 min of incubation. Results indicated that the precipitation of insulin increased with the incubation time in 25, 50, 100, 200 µg/mL of rHaTXNDC17 treated samples. MBP treated samples showed an absorbance similar to the control (0 µg/mL of rHaTXNDC17). DTT-absent treatment did not give a significant absorbance. The IC_{50} values corresponding to 25 µg/mL, 50 µg/mL, 100 µg/mL, and 200 µg/mL were 38.63 ± 0.63, 37.47 ± 0.20, 32.93 ± 0.51, and 27.83 ± 0.21, respectively (Fig. 9). The specific activity was observed at 1.4, 1.9, 2.5, and 2.9 for the 25, 50, 100 and 200 µg/mL concentrations of the rHaTXNDC17 protein, respectively.

3.2.3. Protective effect on the cultured cells under oxidative stress

Toxic effect of H_2O_2 on FHM cells was calculated by MTT assay. According to the results obtained, 88% of live cells were detected among the H_2O_2-treated cells with 0 µg/mL rHaTXNDC17 (Fig. 10). These results showed the peroxidase activity of HaTXNDC17 and its contribution to cell viability upon oxidative stress. Microscopic observations confirmed the cellular protective ability of HaTXNDC17 with respect to different concentrations. H_2O_2 treated cells showed the highest cell damage compared to the untreated cells.

4. Discussion

Thioredoxin and glutathione are two major cellular components mediating the redox balance in cells via cysteine residues. The thioredoxin system includes several isoforms of thioredoxins, thioredoxin reductases, and thioredoxin-dependent proteins [33]. Thioredoxins are involved in various biological processes in prokaryotes as well as eukaryotes [34] and play an important role in regulating the cellular environment by reducing oxidative stress. In this study, the TXNDC17 homolog from the big belly seahorse was characterized, as it may be involved in maintaining redox balance in the seahorse. Several proteins are involved in cellular thiol-redox pathways, including thioredoxin, glutathione S transferase, GRX, and PDI, which are known to adopt a

thioredoxin fold [2,3,8]. Previous subcellular localization studies revealed that TXNDC17 is present in the cytoplasm. Thioredoxins are involved in cellular processes like scavenging radicals in the cellular environment, repairing damaged proteins due to oxidative stress [35], and regulating gene expression and apoptosis [36]. It also modulates the gene expression of tumor necrosis factor and nuclear factor kappa B with dynein light chain LC8 [37,38].

All organisms have different thioredoxin and thioredoxin related isoforms. Conserved CXXC common motif in the thioredoxin domain is essential for the thiol-disulfide reduction in thioredoxin and important in redox balancing in cells [1,33]. HaTXNDC17 has the CXXC motif which is represented by CPDC residues and these residues are conserved in all fish TXNDC17 orthologs. Similar to the other TXNDC17s, HaTXNDC17 was comprised of 123 amino acids. The lack of an *N*-terminal secretory signal indicated the localization of HaTXNDC17 in the cytosol and the lack of *N*-linked glycosylation sites indicated the absence of protein modifications by the Asn residues in the endoplasmic reticulum of eukaryotic cells [39]. According to the protein structure, all thioredoxin isoforms have a similar 3D structure, which consists of five beta strands surrounded by four alpha helixes [25]. The N terminal cysteine of CXXC motif in thioredoxin may be highly conserved and redox-sensitive [8].

HaTXNDC17 is ubiquitously expressed in all of the tissues tested in this experiment as its major function is to maintain cellular redox homeostasis. ROS can interact with biomolecules and cause severe cell damage or cell death [40]. According to the present tissue distribution results, TXNDC17 may actively protect the cells from oxidative damage. Moreover, it helps organs to maintain cellular redox homeostasis and can be found in tissues that are more susceptible to oxidative stress. Muscles are susceptible to higher oxidative stresses due to active swimming in fish species than other tissues [41]. Further, mitochondria produce higher energy to compensate for the energy requirement in brain tissues, which leads to ROS generation. Hence, TXNDC17 plays a crucial role in brain tissues in response to regulate the redox balance [42]. The intestine and stomach of the seahorses abundantly express TXNDC17, which may be due to the microbial flora and by-product accumulation in the digestive system [43]. Therefore, the tissue distribution patterns indicate the involvement of *HaTXNDC17* in cellular defense mechanism.

Considering the immune-related activities of *HaTXNDC17*, the thioredoxin pathway is activated upon pathological stimulation. The upregulation of *HaTXNDC17* expression in the peripheral blood cells after 24–48 h p.i. may be due to an increase in ROS to suppress invading bacteria, like *E. tarda* and *S iniae*. LPS triggers the immune system via the LPS receptors and activates the downstream signaling cascades of macrophages [44]. Poly I:C is a viral mimic that activates the immune response in peripheral blood leukocytes [45]; *HaTXNDC17* may be highly expressed in response to the viral mimic to balance redox stress. Moreover, high oxidative stress occurs in the erythrocytes due to direct interaction with oxygen that leads to ROS generation, and TXNDC17 is actively involved in regulating oxidative stress in blood [46]. Kidney tissues are considered as hematopoietic tissues that are involved in the hematopoiesis process [47,48]. Increased expression of *HaTXNDC17* after 24–48 h may be due to the high amounts of ROS produced during hematopoiesis because of the rapid loss of cells in the host immune system [49]. Further, oxidative stress contributes significantly to hematopoiesis process and erythroid cell formation is sensitive to ROS accumulation [50]. Due to the acute endotoxin stress produced by LPS in the trunk kidney, a high number of immune signaling and apoptosis-related genes were expressed [51] leading to a large amount of ROS in the cells. *HaTXNDC17* was expressed highly in order to regulate the redox stress. Furthermore poly I:C can activate the immune response in kidney macrophages, leading to the activation of downstream signaling cascades [45].

Though members of the thioredoxin family and TXNDC17 are well known to promote redox homeostasis, the function of TXNDC17 is still unclear. Hence, we performed the DPPH radical scavenging assay, insulin reduction assay, and MTT assay to evaluate the function of HaTXNDC17. The DPPH assay is a quite popular assay to measure the antioxidant activity of biological samples [52,53] and DPPH is a highly stable radical-forming agent used to measure the scavenging ability. The color of DPPH changes from purple to yellow according to the antioxidant activity of the compound. Using ascorbic acid as a reference provides the ability to get the absolute IC_{50} value. The IC_{50} of HaTXNDC17 for DPPH can be defined as the concentration of HaTXNDC17 required to inhibit 50% of DPPH radicals, and provides information regarding the potency of HaTXNDC17 in the DPPH radical scavenging activity. According to previous data, the extracellularly acting protein, Mfp-6, is actively involved in capturing free radicals through antioxidant activity [54].

The insulin reduction assay is used to measure the antioxidant ability of proteins where the precipitation of insulin depends on the time of incubation [31]. DTT is a robust reducing agent, and the reduction of the typical disulfide bond is mediated by the sequential thiol-disulfide exchange. Reduction of insulin is facilitated by adding DTT to the mixture and it forms a turbid solution, which can be quantified using spectrophotometry. Thioredoxin promotes the precipitation of insulin while exchanging SH groups with the insulin β chain. Increasing concentration of rHaTXNDC17 logarithmically increases the precipitation of insulin. The rate of precipitation was observed in 200 μg/mL of rHaTXNDC17 as 0.052 min^{-1} and specific activity was observed at 2.93; the specific activity of *L. vannamei* [55], *E. coioides* [56] and *E. sinensis* [57] was observed at 10.44, 6.25, and 5.03, respectively.

The protective ability of rHaTXNDC17 was tested on FHM cells by the MTT assay. Previous studies suggest that TXNDC17 has peroxidase activity [32]. Peroxidases are thiol-dependent proteins that require an electron donor. TXNDC17 has thiol-active cysteine residues that can be activated by electron donors like thioredoxin, GRX, or DTT. The thiol-active CXXC motif undergoes oxidation and reduction in the presence of DTT and H_2O_2. Since TXNDC17 is not a specific enzyme that mediates the cellular peroxidase activity, increasing the concentration of TXNDC17 may not increase cell survival; therefore a linear relationship cannot be observed. The cellular protective ability of peroxidoxin from H_2O_2 was previously studied in *Scophthalmus maximus* [58] and *Haliotis discus discus* [59] to observe peroxidase activity. Microscopic images revealed a reduction in cell growth and damage due to H_2O_2. The HaTXNDC17 treated cells gained the ability to survive under oxidative stress conditions. A previous study on mice peroxidoxin 6 showed significant resistant to H_2O_2 on ketatinocytes [60]. In summary, Cellular ROS level increased during the pathological conditions or oxidative stresses. Hence, the observed results revealed that rHaTXNDC17 may play a significant role in protecting the cellular organelles from H_2O_2-mediated oxidative damage.

5. Conclusion

In conclusion, the *TXNDC17* gene from *H. abdominalis* was analyzed using various *in silico* tools, and the molecular properties were examined. The *HaTXNDC17* gene was ubiquitously expressed in all of the tissues examined. Modulation of *HaTXNDC17* transcripts in peripheral blood cells and trunk kidney revealed significant upregulation against the bacterial and PAMP infections. Furthermore, functional properties such as antioxidant activity, thiol reductase activity, and peroxidase activity of rHaTXNDC17 were observed. These assays showed that rHaTXNDC17 protein served to reduce oxidative stress suggesting that this protein plays a significant role in maintaining cellular defenses against oxidative stress. Moreover, TXNDC17 from *H. abdominalis* was assessed for the first time in this study, and the results provide a better understanding of the functional and molecular properties of the *HaTXNDC17* gene.

Acknowledgment

This research was a part of the project titled 'Fish Vaccine Research Center,' funded by the Ministry of Oceans and Fisheries, Korea and supported by a grant from Marine Biotechnology Program (20180430, Genome Analysis of Marine and Fisheries Organisms and Development of Functional Applications) Funded by Ministry of Oceans and Fisheries, Korea

References

[1] A. Miranda-Vizuete, A.E. Damdimopoulos, J.-Å. Gustafsson, G. Spyrou, Cloning, expression, and characterization of a novel *Escherichia coli* thioredoxin, J. Biol. Chem. 272 (1997) 30841–30847, https://doi.org/10.1074/jbc.272.49.30841.

[2] F. Aslund, B. Ehn, A. Miranda-Vizuete, C. Pueyo, A. Holmgren, Two additional glutaredoxins exist in *Escherichia coli*: glutaredoxin 3 is a hydrogen donor for ribonucleotide reductase in a thioredoxin/glutaredoxin 1 double mutant, Proc. Natl. Acad. Sci. U.S.A. 91 (1994) 9813–9817, https://doi.org/10.1073/pnas.91.21.9813.

[3] G. Kozlov, P. Määttänen, D.Y. Thomas, K. Gehring, A structural overview of the PDI family of proteins, FEBS J. 277 (2010) 3924–3936, https://doi.org/10.1111/j.1742-4658.2010.07793.x.

[4] G. Ren, D. Stephan, Z. Xu, Y. Zheng, D. Tang, R.S. Harrison, M. Kurz, R. Jarott, S.R. Shouldice, A. Hiniker, J.L. Martin, B. Heras, J.C.A. Bardwell, Properties of the thioredoxin fold superfamily are modulated by a single amino acid residue, J. Biol. Chem. 284 (2009) 10150–10159, https://doi.org/10.1074/jbc.M809509200.

[5] H. Nakamura, Thioredoxin and its related molecules: update 2005, Antioxidants Redox Signal. 7 (2005) 823–828, https://doi.org/10.1089/ars.2005.7.823.

[6] A. Holmgren, Thioredoxin, Annu. Rev. Biochem. 54 (1985) 237–271, https://doi.org/10.1146/annurev.bi.54.070185.001321.

[7] F.K. Gleason, A. Holmgren, Thioredoxin and related proteins in procaryotes, FEMS Microbiol. Lett. 54 (1988) 271–297, https://doi.org/10.1016/0378-1097(88)90247-9.

[8] A. Holmgren, Thioredoxin structure and mechanism: conformational changes on oxidation of the active-site sulfhydryls to a disulfide, Structure 3 (1995) 239–243, https://doi.org/10.1016/S0969-2126(01)00153-8.

[9] A. Holmgren, M. Bjornstedt, Thioredoxin and thioredoxin reductase, Methods Enzymol. 252 (1995) 199–208, https://doi.org/10.1016/0076-6879(95)52023-6.

[10] L.M. Landino, T.E. Skreslet, J.A. Alston, Cysteine oxidation of tau and microtubule-associated protein-2 by peroxynitrite: modulation of microtubule assembly kinetics by the thioredoxin reductase system, J. Biol. Chem. 279 (2004) 35101–35105, https://doi.org/10.1074/jbc.M405471200.

[11] J. Messens, S. Silver, Arsenate reduction: thiol cascade chemistry with convergent evolution, J. Mol. Biol. 362 (2006) 1–17, https://doi.org/10.1016/j.jmb.2006.07.002.

[12] R. Kern, A. Malki, A. Holmgren, G. Richarme, Chaperone properties of *Escherichia coli* thioredoxin and thioredoxin reductase, Biochem. J. 371 (2003) 965–972, https://doi.org/10.1042/bj20030093.

[13] T. Nakamura, H. Nakamura, T. Hoshino, S. Ueda, H. Wada, J. Yodoi, Redox regulation of lung inflammation by thioredoxin, Antioxid. Redox Signal. 7 (2005) 60–71, https://doi.org/10.1089/ars.2005.7.60.

[14] D. Ravi, H. Muniyappa, K.C. Das, Endogenous thioredoxin is required for redox cycling of anthracyclines and p53-dependent apoptosis in cancer cells, J. Biol. Chem. 280 (2005) 40084–40096, https://doi.org/10.1074/jbc.M507192200.

[15] C.H. Chang, N.H. Jang-Liaw, Y.S. Lin, Y.C. Fang, K.T. Shao, Authenticating the use of dried seahorses in the traditional Chinese medicine market in Taiwan using molecular forensics, J. Food Drug Anal. 21 (2013) 310–316, https://doi.org/10.1016/jjfda.2013.07.010.

[16] A.C.J. Vincent, S.J. Foster, H.J. Koldewey, Conservation and management of seahorses and other Syngnathidae, J. Fish. Biol. 78 (2011) 1681–1724, https://doi.org/10.1111/j.1095-8649.2011.03003.x.

[17] J.L. Balcázar, A. Gallo-Bueno, M. Planas, J. Pintado, Isolation of *Vibrio alginolyticus* and *Vibrio splendidus* from captive-bred seahorses with disease symptoms, Antonie van Leeuwenhoek, Int. J. Gen. Mol. Microbiol. 97 (2010) 207–210, https://doi.org/10.1007/s10482-009-9398-4.

[18] A.C.J. Vincent, R.S. Clifton-Hadley, Parasitic infection of the seahorse (*Hippocampus erectus*)— a case report, J. Wildl. Dis. 25 (1989) 404–406, https://doi.org/10.7589/0090-3558-25.3.404.

[19] *Hippocampus* spp (Seahorses), CITES, (n.d.). https://cites.org/eng/taxonomy/term/331 (accessed March 31, 2018).

[20] S. Bin Park, T. Aoki, T.S. Jung, Pathogenesis of and strategies for preventing *Edwardsiella tarda* infection in fish, Vet. Res. 43 (2012) 67, https://doi.org/10.1186/1297-9716-43-67.

[21] M.R. Weinstein, M. Litt, D.A. Kertesz, P. Wyper, D. Rose, M. Coulter, A. McGeer, R. Facklam, C. Ostach, B.M. Willey, A. Borczyk, D.E. Low, Invasive infections due to a fish pathogen, *Streptococcus iniae*, N. Engl. J. Med. 337 (1997) 589–594, https://doi.org/10.1056/NEJM199708283370902.

[22] T.T. Priyathilaka, M. Oh, S.D.N.K. Bathige, M. De Zoysa, J. Lee, Two distinct CXC chemokine receptors (CXCR3 and CXCR4) from the big-belly seahorse *Hippocampus abdominalis*: molecular perspectives and immune defensive role upon pathogenic stress, Fish Shellfish Immunol. 65 (2017) 59–70, https://doi.org/10.1016/j.fsi.2017.03.038.

[23] E. Jo, D.A.S. Elvitigala, Q. Wan, M. Oh, C. Oh, J. Lee, Identification and molecular profiling of DC-SIGN-like from big belly seahorse (*Hippocampus abdominalis*) inferring its potential relevancy in host immunity, Dev. Comp. Immunol. 77 (2017) 270–279, https://doi.org/10.1016/j.dci.2017.08.017.

[24] M. Oh, N. Umasuthan, D.A.S. Elvitigala, Q. Wan, E. Jo, J. Ko, G.E. Noh, S. Shin, S. Rho, J. Lee, First comparative characterization of three distinct ferritin subunits from a teleost: evidence for immune-responsive mRNA expression and iron depriving activity of seahorse (*Hippocampus abdominalis*) ferritins, Fish Shellfish Immunol. 49 (2016) 450–460, https://doi.org/10.1016/j.fsi.2015.12.039.

[25] R. Agarwala, T. Barrett, J. Beck, D.A. Benson, C. Bollin, E. Bolton, D. Bourexis, J.R. Brister, S.H. Bryant, K. Canese, C. Charowhas, K. Clark, M. Dicuccio, I. Dondoshansky, S. Federhen, M. Feolo, K. Funk, L.Y. Geer, V. Gorelenkov, M. Hoeppner, B. Holmes, M. Johnson, V. Khotomlianski, A. Kimchi, M. Kimelman, P. Kitts, W. Klimke, S. Krasnov, A. Kuznetsov, M.J. Landrum, D. Landsman, J.M. Lee, D.J. Lipman, Z. Lu, T.L. Madden, T. Madej, A. Marchler-Bauer, I. Karsch-Mizrachi, T. Murphy, R. Orris, J. Ostell, C. O'sullivan, A. Panchenko, L. Phan, D. Preuss, K.D. Pruitt, K. Rodarmer, W. Rubinstein, E. Sayers, V. Schneider, G.D. Schuler, S.T. Sherry, K. Sirotkin, K. Siyan, D. Slotta, A. Soboleva, V. Soussov, G. Starchenko, T.A. Tatusova, K. Todorov, B.W. Trawick, D. Vakatov, Y. Wang, M. Ward, W.J. Wilbur, E. Yaschenko, K. Zbicz, Database resources of the national center for Biotechnology information, Nucleic Acids Res. 44 (2016) D7–D19, https://doi.org/10.1093/nar/gkv1290.

[26] S. Kumar, G. Stecher, K. Tamura, MEGA7: molecular evolutionary Genetics analysis version 7.0 for bigger datasets, Mol. Biol. Evol. 33 (2016) 1870–1874, https://doi.org/10.1093/molbev/msw054.

[27] K.J. Livak, T.D. Schmittgen, Analysis of relative gene expression data using real-time quantitative PCR and the 2-ΔΔCT method, Methods 25 (2001) 402–408, https://doi.org/10.1006/meth.2001.1262.

[28] S. Qi, B. Zhao, B. Zhou, X. Jiang, An electrochemical immunosensor based on pristine graphene for rapid determination of ractopamine, Chem. Phys. Lett. 685 (2017) 146–150, https://doi.org/10.1016/j.cplett.2017.07.055.

[29] V.K. Bajpai, A. Sharma, S.C. Kang, K.H. Baek, Antioxidant, lipid peroxidation inhibition and free radical scavenging efficacy of a diterpenoid compound sugiol isolated from *Metasequoia glyptostroboides*, Asian Pac. J. Trop. Med. 7 (2014) 9–15, https://doi.org/10.1016/S1995-7645(13)60183-2.

[30] J.L. Sebaugh, Guidelines for accurate EC50/IC50 estimation, Pharmaceut. Stat. 10 (2011) 128–134, https://doi.org/10.1002/pst.426.

[31] A. Holmgren, Thioredoxin catalyzes the reduction of insulin disulfides by dithiothreitol and dihydrolipoamide, J. Biol. Chem. 254 (1979) 9627–9632 doi:10.10.79.

[32] K. Hirota, H. Nakamura, H. Masutani, J. Yodoi, Thioredoxin superfamily and thioredoxin-inducing agents, Ann. N. Y. Acad. Sci. 957 (2002) 189–199, https://doi.org/10.1111/j.1749-6632.2002.tb02916.x.

[33] E.S.J. Arnér, A. Holmgren, Physiological functions of thioredoxin and thioredoxin reductase, Eur. J. Biochem. 267 (2000) 6102–6109, https://doi.org/10.1046/j.1432-1327.2000.01701.x.

[34] M.H. Glickman, A. Ciechanover, The ubiquitin-proteasome proteolytic pathway: destruction for the sake of construction, Physiol. Rev. 82 (2002) 373–428, https://doi.org/10.1152/physrev.00027.2001.

[35] M.R. Fernando, H. Nanri, S. Yoshitake, K. Nagata-Kuno, S. Minakami, Thioredoxin regenerates proteins inactivated by oxidative stress in endothelial cells, Eur. J. Biochem. 209 (1992) 917–922, https://doi.org/10.1111/j.1432-1033.1992.tb17363.x.

[36] M. Saitoh, H. Nishitoh, M. Fujii, K. Takeda, K. Tobiume, Y. Sawada, M. Kawabata, K. Miyazono, H. Ichijo, Mammalian thioredoxin is a direct inhibitor of apoptosis signal-regulating kinase (ASK) 1, EMBO J. 17 (1998) 2596–2606, https://doi.org/10.1093/emboj/17.9.2596.

[37] J.R. Woo, S.J. Kim, W. Jeong, Y.H. Cho, S.C. Lee, Y.J. Chung, S.G. Rhee, S.E. Ryu, Structural basis of cellular redox regulation by human TRP14, J. Biol. Chem. 279 (2004) 48120–48125, https://doi.org/10.1074/jbc.M407079200.

[38] W. Jeong, T.S. Chang, E.S. Boja, H.M. Fales, S.G. Rhee, Roles of TRP14, a thioredoxin-related protein in tumor necrosis factor-α signaling pathways, J. Biol. Chem. 279 (2004) 3151–3159, https://doi.org/10.1074/jbc.M307959200.

[39] S. Ranganathan, S. Wongsai, K.M.H. Nevalainen, Comparative genomic analysis of glycoylation pathways in yeast, plants and higher eukaryotes, Appl. Mycol. Biotechnol. 6 (2006) 227–248, https://doi.org/10.1016/S1874-5334(06)80013-4.

[40] E. Birben, U.M. Sahiner, C. Sackesen, S. Erzurum, O. Kalayci, Oxidative stress and antioxidant defense, World Allergy Organ. J. 5 (2012) 9–19, https://doi.org/10.1097/WOX.0b013e3182439613.

[41] D.W. Filho, Reactive oxygen species, antioxidants and fish mitochondria, Front. Biosci. 12 (2007) 1229, https://doi.org/10.2741/2141.

[42] A. Meister, Metabolism and functions of glutathione, Trends Biochem. Sci. 6 (1981) 231–234, https://doi.org/10.1016/0968-0004(81)90084-0.

[43] A. Bhattacharyya, R. Chattopadhyay, S. Mitra, S.E. Crowe, Oxidative stress: an essential factor in the pathogenesis of gastrointestinal mucosal diseases, Physiol. Rev. 94 (2014) 329–354, https://doi.org/10.1152/physrev.00040.2012.

[44] T. Ki, T.S. Hade, U.W.E. Mamai, G. Nter, H. Brade, H. Loepno, F.O.D.I. Pava, Activity endotoxin : mOle ..: ar ships of struetui to and fction ; L0M, FASEB J. 8 (1994) 217–225 http://www.ncbi.nlm.nih.gov/pubmed/8119492.

[45] Z. Zhou, B. Zhang, L. Sun, Poly(I:C) induces antiviral immune responses in Japanese Flounder (*Paralichthys olivaceus*) that require TLR3 and MDA5 and is negatively regulated by Myd88, PLoS One 9 (2014) e112918, , https://doi.org/10.1371/journal.pone.0112918.

[46] G.C. Mills, Hemoglobin catabolism, J. Biol. Chem. 229 (1957) 189–197 http://www.jbc.org/cgi/content/short/229/1/189.

[47] W.T. Catton, Blood cell formation in certain teleost fishes, Blood 6 (2012) 39–60 http://www.bloodjournal.org/content/6/1/39?sso-checked=true.

[48] R.J. Roberts, A.E. Ellis, The anatomy and physiology of teleosts, Fish Pathol. fourth

ed., Wiley-Blackwell, Oxford, UK, 2012, pp. 17–61, , https://doi.org/10.1002/9781118222942.ch2.
[49] M. Sattler, T. Winkler, S. Verma, C.H. Byrne, G. Shrikhande, R. Salgia, J.D. Griffin, Hematopoietic growth factors signal through the formation of reactive oxygen species, Blood 93 (1999) 2928–2935 http://www.ncbi.nlm.nih.gov/pubmed/10216087.
[50] S. Ghaffari, Oxidative stress in the regulation of normal and neoplastic hematopoiesis, Antioxidants Redox Signal. 10 (2008) 1923–1940, https://doi.org/10.1089/ars.2008.2142.
[51] G. Forn-Cuní, M. Varela, P. Pereiro, B. Novoa, A. Figueras, Conserved gene regulation during acute inflammation between zebrafish and mammals, Sci. Rep. 7 (2017), https://doi.org/10.1038/SREP41905.
[52] Dejian Huang, Boxin Ou, R.L. Prior, The Chemistry behind Antioxidant Capacity Assays, (2005), https://doi.org/10.1021/JF030723C.
[53] M. Antolovich, P.D. Prenzler, E. Patsalides, S. McDonald, K. Robards, Methods for testing antioxidant activity, Analyst 127 (2002) 183–198 http://www.ncbi.nlm.nih.gov/pubmed/11827390.
[54] H. Zhao, J.H. Waite, Linking adhesive and structural proteins in the attachment plaque of *Mytilus californianus*, J. Biol. Chem. 281 (2006) 26150–26158, https://doi.org/10.1074/jbc.M604357200.
[55] E. Aispuro-Hernandez, K.D. Garcia-Orozco, A. Muhlia-Almazan, L. Del-Toro-Sanchez, R.M. Robles-Sanchez, J. Hernandez, G. Gonzalez-Aguilar, G. Yepiz-Plascencia, R.R. Sotelo-Mundo, Shrimp thioredoxin is a potent antioxidant protein, Comp. Biochem. Physiol. C Toxicol. Pharmacol. 148 (2008) 94–99, https://doi.org/10.1016/j.cbpc.2008.03.013.
[56] J. Wei, M. Guo, H. Ji, Y. Yan, Z. Ouyang, X. Huang, Y. Hang, Q. Qin, Cloning, characterization, and expression analysis of a thioredoxin from orange-spotted grouper (*Epinephelus coioides*), Dev. Comp. Immunol. 38 (2012) 108–116, https://doi.org/10.1016/j.dci.2012.04.011.
[57] C. Mu, J. Zhao, L. Wang, L. Song, X. Song, H. Zhang, L. Qiu, Y. Gai, Z. Cui, A thioredoxin with antioxidant activity identified from *Eriocheir sinensis*, Fish Shellfish Immunol. 26 (2009) 716–723, https://doi.org/10.1016/j.fsi.2009.02.024.
[58] W.J. Zheng, Y.H. Hu, M. Zhang, L. Sun, Analysis of the expression and antioxidative property of a peroxiredoxin 6 from *Scophthalmus maximus*, Fish Shellfish Immunol. 29 (2010) 305–311, https://doi.org/10.1016/j.fsi.2010.04.008.
[59] C. Nikapitiya, M. De Zoysa, I. Whang, C.G. Kim, Y.H. Lee, S.J. Kim, J. Lee, Molecular cloning, characterization and expression analysis of peroxiredoxin 6 from disk abalone *Haliotis discus discus* and the antioxidant activity of its recombinant protein, Fish Shellfish Immunol. 27 (2009) 239–249, https://doi.org/10.1016/j.fsi.2009.05.002.
[60] A. Kümin, C. Huber, T. Rülicke, E. Wolf, S. Werner, Peroxiredoxin 6 is a potent cytoprotective enzyme in the epidermis, Am. J. Pathol. 169 (2006) 1194–1205, https://doi.org/10.2353/ajpath.2006.060119.